Phosphate Release during Microtubule Assembly: What Stabilizes Growing Microtubules?†

André Vandecandelaere, Martin Brune, Martin R. Webb, Stephen R. Martin, and Peter M. Bayley*

Division of Physical Biochemistry, National Institute for Medical Research, The Ridgeway, Mill Hill, London NW7 1AA, U.K.

Received December 30, 1998; Revised Manuscript Received April 20, 1999

ABSTRACT: The molecular mechanism underlying microtubule dynamic instability depends on the relationship between the addition of tubulin-GTP to a growing microtubule and its hydrolysis in the microtubule lattice to tubulin-GDP, with release of inorganic phosphate (P_i). Since this relationship remains controversial, we have re-examined the release of P_i upon microtubule assembly using a fluorometric assay for P_i, based on the phosphate-binding protein of *Escherichia coli* [Brune M., Hunter, J. L., Corrie, J. E. T., and Webb, M. R. (1994) *Biochemistry 33*, 8262−8271]. Microtubule assembly and P_i release were monitored simultaneously in a standard fluorimeter as an increase in the turbidity and fluorescence, respectively, in tubulin-GTP solutions assembled under conditions supporting dynamic instability. At the steady state of assembly, P_i release is nonlinear with respect to time, proceeding at a rate determined by the following: (a) the intrinsic GTPase activity of the nonpolymerized tubulin-GTP, and (b) the microtubule number concentration, which decreases progressively. Direct observation of the time course of nucleated microtubule assembly indicates that P_i release is closely coupled to microtubule elongation, even during the initial stages of assembly when uncoupling of tubulin-GTP addition and GTP hydrolysis would be most evident. Studies of the inhibition and reversal of the growth phase by cytostatic drugs show no evidence of a burst of P_i release. We conclude that nucleotide hydrolysis can keep pace with tubulin-GTP addition rates of 200 molecules per second per microtubule and that extended caps of tubulin-GTP or tubulin-GDP−P_i are not generated in normal assembly, nor are they required to stabilize growing microtubules or to support the phenomenon of dynamic instability of microtubules at the steady state.

Microtubules are major components of the eukaryotic cytoskeleton and play important roles in many cellular functions, such as mitosis and meiosis, intracellular transport, cell motility, and cell-shape determination. They are produced by the polymerization of tubulin, a 100 kDa $\alpha\beta$-heterodimer with binding sites for guanosine nucleotides and cytostatic drugs, including colchicine, podophyllotoxin, vinblastine, and taxol. Microtubules are cylindrical polymers (24 nanometers in diameter, several micrometers long), in which the tubulin subunits are arranged longitudinally in protofilaments (generally 13−14) (for general references, see refs *1*−*3*).

One of the most remarkable properties of microtubules is their ability, under appropriate conditions, to display "dynamic instability" behavior, whereby they undergo random transitions between periods of slow growth and ∼10-fold faster shortening (*4*, *5*). It is generally accepted that this behavior is related to the hydrolysis of GTP which is usually required to assemble tubulin. Microtubules assembled in the presence of non- (or slowly) hydrolyzable GTP analogues do not display dynamic instability (*6*−*8*). In addition, the normal microtubule lattice is a kinetically heterogeneous structure, the dissociation rate constant for tubulin-GDP (Tu-GDP)[1] from the lattice being significantly larger than that for Tu-GTP (*6*, *9*, *10*). Earlier reports suggested that the hydrolysis of GTP follows the addition of Tu-GTP with a considerable delay (*11*, *12*). Consequently, microtubules are generally considered as intrinsically unstable polymers consisting largely of Tu-GDP, containing a stabilizing structure of some sort at their ends.

Although the causal relationship between the hydrolysis of nucleotide and the dynamic properties of microtubules is not in doubt, the precise relationship between the addition of Tu-GTP, the hydrolysis of the nucleotide and, hence, the nature of the putative stabilizing structure at the ends remains unresolved. Three experimental approaches have been used to address this issue. (1) The release of P_i has been monitored during microtubule assembly, usually using [γ-^{32}P]GTP. P_i release was first reported to follow assembly with a considerable delay in the presence of high [Mg^{2+}] (6 mM)

† This work was supported by the Medical Research Council, United Kingdom.

* Corresponding author. Tel: + 44 181 959 3666 Fax: + 44 181 906 4477. E-mail: p-bayley@nimr.mrc.ac.uk.

[1] Abbreviations: PBP, phosphate binding protein; MDCC, *N*-[2-(1-maleimidyl)ethyl]-7-diethylamino)coumarin-3-carboxamide; MDCC−PBP, A197C mutant of PBP labeled with MDCC; MTC, 2-methoxy-5-(2′,3′,4′-trimethoxyphenyl) tropone; Tu-GTP (Tu-GDP), the tubulin $\alpha\beta$-heterodimer with GTP (GDP) at the exchangeable nucleotide binding site (E-site); MAPs, microtubule associated proteins; Pipes, 1,4-piperazinediethane-sulfonate; EGTA, ethylene glycol-bis(β-aminoethyl ether) *N*,*N*,*N*′,*N*′-tetraacetic acid; PEM, microtubule assembly buffer containing 100 mM Pipes, 1 mM EGTA, and 0.5 mM $MgCl_2$ at pH 6.5; PEMG, PEM buffer containing 1 M glycerol; C_t, the total concentration of tubulin; C_c, the critical concentration; C_s, the concentration of tubulin in the soluble phase; C_p, the concentration of tubulin in the polymeric phase; C_n, the microtubule number concentration.

10.1021/bi9830765 CCC: $18.00
Published on Web 06/04/1999

and 3.4 M glycerol (*11*, *12*). A subsequent report (*13*) failed to confirm such a delay in assembly buffer containing only 1 mM Mg^{2+} and no glycerol, indicating that P_i release and microtubule assembly are coupled. Recently, using an enzyme-linked P_i assay Melki et al. (*14*) observed a (small) delay in P_i release relative to assembly under conditions of very fast, irreversible, taxol-induced assembly. (2) In another approach, the appearance of GDP in microtubules was compared with microtubule assembly (*13*, *15*−*19*). This approach invariably failed to detect appreciable amounts of GTP in the polymer. (3) By using the slowly hydrolyzing GTP analogue, guanylyl-(α*β*)-methylene-diphosphonate (GMPCPP) (*20*, *21*), it was estimated by optical microscopy that ∼13 Tu-GTPs per microtubule end, that is, one at the end of each protofilament, are sufficient to stabilize the entire lattice at the steady state of assembly. There is, therefore, considerable evidence to support the view that hydrolysis of the nucleotide is closely coupled to the addition of Tu-GTP.

On the basis of the original deduction of delayed P_i release, models have been developed including the possibility of large "GTP-caps" (i.e., extensive longitudinal stretches of Tu-GTP at the microtubule ends) which are assumed to stabilize the Tu-GDP lattice (*22*). Given the failure to detect appreciable amounts of GTP in the microtubules, an alternative model (the lateral cap model) has been developed as the limiting case of coupled hydrolysis in which the stabilizing structure is confined to a single terminal layer of Tu-GTP (*23*−*25*). Both models specify kinetic constants which enable extensive numerical simulation of microtubule dynamics. A further mechanism has been proposed which attributes a stabilizing effect to Tu-GDP−P_i (rather than Tu-GTP) in the microtubule end (*26*, *27*). This model postulates delayed release of P_i, on the basis of the observation that fluoride complexes of Be^{2+} and Al^{3+} have a stabilizing effect on the microtubules. BeF_3^- and AlF_4^- are considered to be analogues of P_i, and the related complexes have been considered to be transition-state analogues in a number of nucleotide triphosphate enzymic reactions. On the other hand, observations made by video microscopy failed to show a stabilizing effect on the microtubules of added P_i (*28*, *29*). Recently, the disassembly rate of microtubules was found to be unaffected by added P_i, and this work also questioned whether the metal fluorides are kinetically appropriate analogues of P_i (*30*). At the same time, it has been reported that up to 6% of yeast tubulin in assembled microtubules contains GTP or P_i at the exchangeable site (*31*). Hence the possible role of GDP−P_i in stabilizing growing microtubules remains controversial.

The current uncertainty about the detailed relationship between the addition of Tu-GTP, the hydrolysis of the nucleotide, and the release of P_i profoundly affects the present understanding of microtubule dynamics. In the present work, we have therefore re-examined the relationship between P_i release and microtubule assembly using a new phosphate assay (*32*, *33*). The assay makes use of a P_i-induced change in the fluorescence of the A197C mutant of the phosphate-binding protein from *Escherichia coli*, labeled with *N*-[2-(1-maleimidyl)ethyl]-7-(diethylamino)coumarin-3-carboxamide (MDCC). The affinity of this MDCC−PBP for P_i is high ($K_d \sim 0.1$ μM), the binding is fast ($k_{assoc} \sim 10^8$ M^{-1} s^{-1}), and the interaction with P_i produces a >5-fold increase in fluorescence intensity (*33*). This allows the continuous monitoring of the release of P_i at good time resolution, with simultaneous monitoring of turbidity as an assay of microtubule assembly, and without having to disturb the solution for sampling in order to separate reaction products. It is shown that, while the major contribution to P_i release is from microtubule elongation, the GTPase activity of the Tu-GTP, which can be significant under certain conditions, complicates the quantitative analysis. The results support the view that assembly and GTP hydrolysis are effectively coupled, even at the initial stage of fast nucleated assembly, when uncoupling would be most evident. GTP hydrolysis is clearly able to keep pace with Tu-GTP addition rates of more than 200 tubulins per second per microtubule under conditions supporting microtubule dynamic instability.

EXPERIMENTAL PROCEDURES

Materials. Tubulin was isolated from porcine brain by repeated cycles of assembly and disassembly (*34*), separated from microtubule associated proteins (MAPs) by chromatography on Whatman P11 phosphocellulose (*35*), and stored at −80 °C in 100 mM Pipes, 1 mM EGTA, 5 mM $MgCl_2$, and 3.4 M glycerol (pH 6.5). Before each experiment an additional cycle of assembly and disassembly was used to remove inactive material. The tubulin was then incubated with 1 mM GTP and passed through a PD-10 column (Pharmacia) to remove excess nucleotide. Tubulin and guanosine nucleotide concentrations were determined as described (*36*). The critical concentration (C_c) and inactive protein fraction (f_i) were determined for each tubulin preparation as follows: Tu-GTP (30 μM) was assembled at 37 °C in PEMG buffer with 250 μM GTP. At the steady state of assembly, aliquots of this solution were diluted to different total concentrations (C_t). After re-establishment of the steady state, microtubules were separated from soluble tubulin by ultracentrifugation (15 min at 30000*g*, *k*-factor = 77.8). The tubulin concentration in the supernatant (C_s) was measured by the method of Bradford (*37*), and C_c and f_i were determined as the intercept and slope of a plot of C_s against C_t (see Figure 1).

Microtubule fragments for seeded-assembly studies were prepared immediately prior to each experiment. Tu-GTP (25 μM) was incubated in PEMG buffer at 37 °C, and fast assembly was initiated by the addition of a stoichiometric amount of paclitaxel (taxol, Fluka) or by addition of 10% (v/v) dimethylsulfoxide (DMSO). The mixture was incubated at 37 °C for a further 13 min before addition to the experimental system. No significant differences were observed between assemblies induced with the different seed preparations.

MDCC−PBP was prepared and characterized as described (*32*, *33*). The response of MDCC−PBP to P_i addition under different buffer conditions was calibrated using a commercially available P_i standard (Merck).

Simultaneous Monitoring of Microtubule Assembly and the Release of P_i. Tu-GTP was mixed on ice with MDCC−PBP in PEMG buffer, degassed, and placed in a 3 × 3 mm fluorescence cuvette. The assembly reaction was monitored at 37 °C under conditions of self-assembly or nucleation by seeds. Microtubule assembly and the release of P_i were monitored in a SPEX FluoroMax fluorimeter. The emission wavelength was set at 465 nm (the fluorescence emission

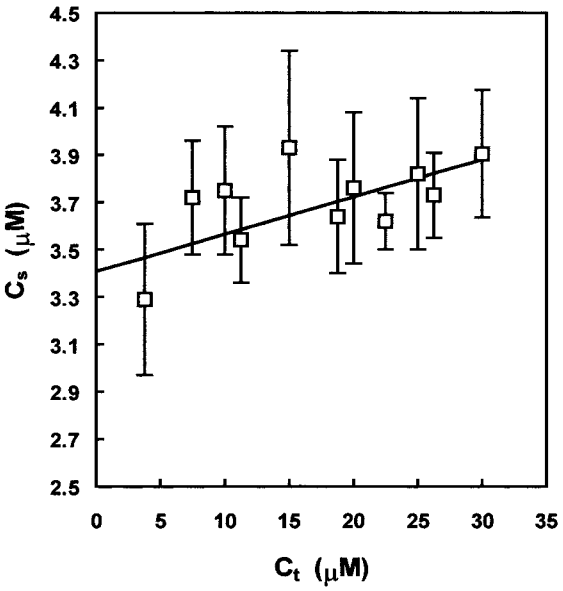

FIGURE 1: Determination of the critical concentration (C_c) and fraction of inactive protein (f_i) for a typical tubulin preparation. Preassembled microtubules were incubated at different total tubulin concentrations (C_t) and separated from soluble tubulin by ultracentrifugation. The concentration of tubulin in the supernatant (C_s) is plotted against C_t, giving an apparent C_c of 3.4 ± 0.6 μM as the intercept and f_i = 0.016 ± 0.013 as the slope. Each point is the average of between three and five determinations.

maximum for MDCC−PBP−P_i); the excitation monochromator was alternated between 425 nm (the isobestic point in the absorption spectra of MDCC−PBP and MDCC−PBP.P_i) for fluorescence and 465 nm for 90° light-scattering measurements. The time lapse between measuring the scattered light, $I_{90}(t)$ and the fluorescent light, $F_{465}(t)$, was 0.2 s, and readings were typically taken at 1 s intervals. The dependence of the total light-scattering intensity $\Delta I_{90}(\infty)$ (equal to $I_{90}(\infty) - I_{90}(0)$) on the steady-state polymer mass $C_p(\infty)$ (calculated from C_t and the C_c corrected for the fraction of inactive tubulin) was linear with a slope of (353 ± 32) × 10^5 cps μM^{-1} (data not shown). In a particular assembly experiment, the polymer mass at any time is calculated using $C_p(t) = C_p(\infty)[I_{90}(t) - I_{90}(0)]/\Delta I_{90}(\infty)$.

At the end of the elongation phase of assembly, and at longer times during the steady state, samples were taken for the determination of microtubule number concentrations from length measurements. These measurements were made using previously described methods of fixation (*38*). Consistency of seeding was checked from successive assemblies at a given tubulin concentration, and seed number concentrations were determined directly.

Quantitative Analysis of MT Assembly and P_i Release. Light-scattering curves for seeded microtubule assembly were analyzed using the following simplified model. The microtubule number concentration (C_n) remains constant during the elongation phase of assembly, and the increase in polymer mass is therefore given by the following:

$$C_p(t) = C_p(\infty)[1 - \exp(-k_{obs}t)] \quad (1)$$

where k_{obs} is the observed rate for assembly (Note: $k_{obs} = k_a C_n$, where k_a is the effective bimolecular rate constant for the addition of Tu-GTP to microtubule ends). This analysis assumes that the fraction of growing microtubules (f_G) remains constant over the entire time course. Under conditions supporting dynamic instability, the value of f_G may be expected to fall to ~0.9 as the steady state is approached (*25*).

P_i is released by two processes: (1) Spontaneous hydrolysis of GTP bound to soluble tubulin: rate = $R_{Pi,Int} = k_{Int}C_s(t)$, where $C_s(t)$ is the concentration of soluble tubulin at time t and k_{Int} is the first-order rate constant for intrinsic hydrolysis. (2) GTP hydrolysis related to microtubule elongation: If this is directly coupled to the bimolecular addition reaction (rate = $k_a f_G C_s(t) C_n$) and P_i is not retained in the lattice, the total rate of P_i release can be expressed as follows:

$$d[P_i]/dt = k_a f_G C_s(t) C_n + k_{Int} C_s(t) \quad (2)$$

Equation 2 can be integrated using the simplifying assumption that $f_G = 1$ to yield the following:

$$[P_i](t) = C_p(\infty)(k'/k_{obs})(1 - \exp(-k_{obs}t)) + k'C_c t + P_i(0) \quad (3)$$

where $k' = k_{obs} + k_{Int}$ and $P_i(0)$ is the background P_i concentration prior to the start of assembly. Thus, on this assumption, the time dependence of P_i release is expected to be given by an exponential function plus a linear background. Observed rates for microtubule assembly, k_{obs}, were obtained using eq 1. The same value could, in principle, be obtained through analysis of the fluorescence signal using eq 3, but in practice (see Results), the background signal (initially a constant slope equal to $k'C_c$) deviates from linearity at longer times. Several effects may contribute to this; for example, dynamic instability results in a decrease in the microtubule number concentration (and therefore k') after extended periods at the steady state, and GDP release may affect steady-state kinetics (*38*). At the steady state of assembly, $C_s(t) = C_c$, and eq 2 reduces to the following:

$$d[P_i]/dt(\text{steady state}) = R_{Pi,Total} = R_{Pi,DI} + R_{Pi,Int}$$

where $R_{Pi,DI}$ (= $k_a f_G C_c C_n$) is the rate for P_i production associated with dynamic instability (DI) due to monomer−polymer exchange reactions at the steady state.

RESULTS

The Intrinsic GTPase of Tubulin Subunits. It is well-established that tubulin has a significant GTPase activity, independent of the reaction with microtubule ends (*39*−*41*). A complete understanding of the P_i release curves obtained under conditions supporting microtubule assembly requires knowledge of the rate of this intrinsic GTPase activity ($R_{Pi,Int}$). We have therefore used MDCC−PBP to measure the rate of P_i production in PEMG buffer at 37 °C under nonassembly conditions. Fluorescence changes were recorded following the addition of Tu-GTP (C_t = 1−30 μM) and MDCC−PBP (20−80 μM) to a prewarmed cuvette (Figure 2A). The decrease in the fluorescence signal in the first 100 s is due to temperature equilibration. For C_t < 20 μM, P_i release is linear with time and the rates obtained ($R_{Pi,Int}$, Figure 2B) agree reasonably well with those obtained under various conditions by Caplow and Shanks (*39*) (0.6 nM s^{-1} at C_t = 2.7 μM) and by Carlier et al. (*41*) (1.7 nM s^{-1} at C_t = 10.0

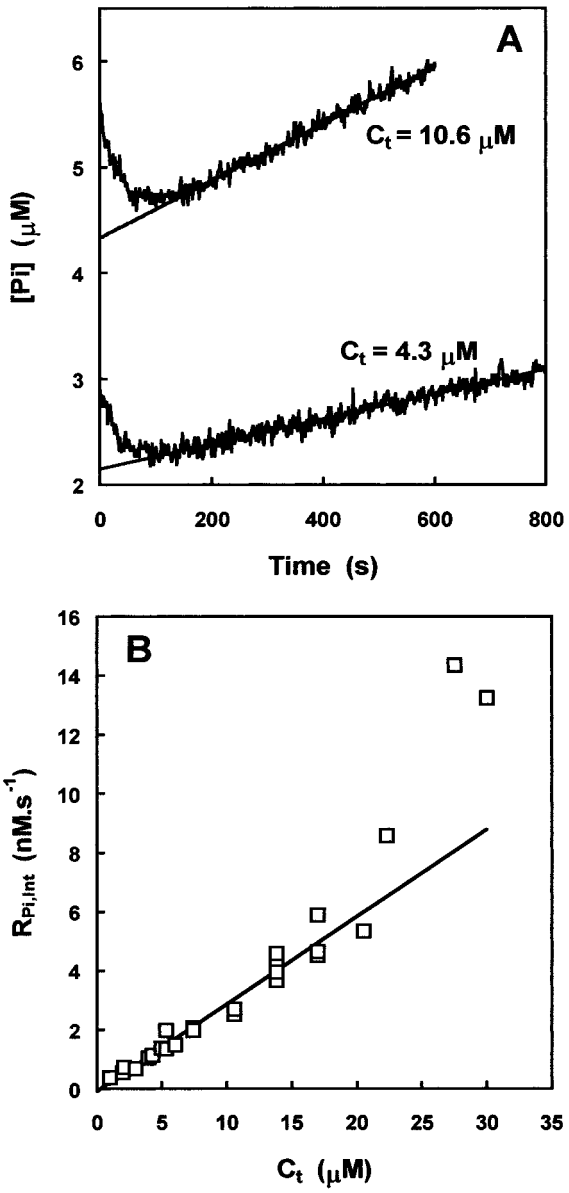

FIGURE 2: The intrinsic GTPase of Tu-GTP. (A) Typical curves showing P_i production as a function of time for two concentrations of Tu-GTP. The slopes of these curves (t > 200 s) give the rates for the intrinsic GTPase ($R_{Pi,Int}$). (B) The rate of the intrinsic GTPase ($R_{Pi,Int}$) as a function of the Tu-GTP concentration (C_t). Linear regression to these data (C_t < 20 μM) gives the first-order rate constant (k_{Int}) for the intrinsic GTPase of 2.9 × 10^{-4} nM s^{-1}.

μM). A plot of $R_{Pi,Int}$ as a function of C_t is linear at C_t < 20 μM (Figure 2B), and a linear fit over this concentration range gave a first-order rate constant, k_{Int}, of 2.9 (± 0.01) × 10^{-4} s^{-1}. At C_t > 20 μM the rate of P_i production only remains constant for a short period prior to the onset of self-assembly. However, the rates for P_i production obtained at C_t > 20 μM are significantly higher than the linear relationship, indicating a significant contribution to P_i production from nucleation or prenucleation events, as deduced by Carlier et al. (*41*). The important result is that, under most conditions, the amount of P_i produced through the intrinsic GTPase of tubulin is small compared with that produced through microtubule elongation, both during the elongation phase and at the steady state (see below). We have therefore assumed a linear dependence in further analysis and used k_{Int} = 2.9 × 10^{-4} s^{-1} in all calculations.

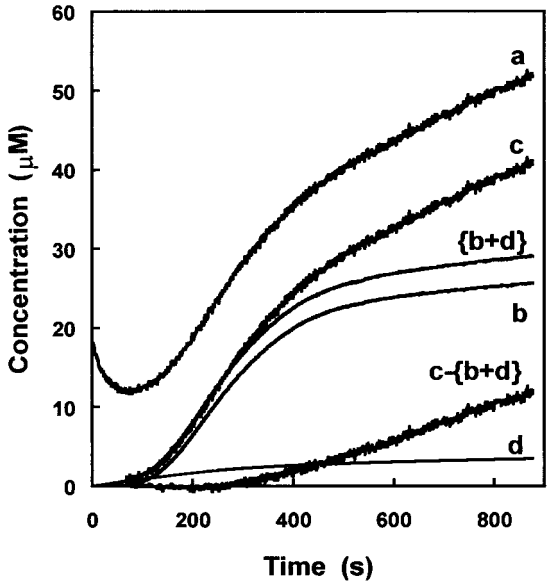

FIGURE 3: P_i release under self-assembly conditions. Fluorescence and light-scattering signals were monitored following the addition of Tu-GTP (30 μM), MDCC−PBP (90 μM), and excess GTP (120 μM) in PEMG buffer to a prewarmed (37 °C) cuvette. The curves are labeled as follows: (a) measured P_i concentration; (b) concentration of tubulin present as polymer (C_p); (c) P_i release curve (curve a corrected for P_i background); and (d) P_i production from the intrinsic GTPase of Tu-GTP. The sum curve ({b + d}) represents the amount of P_i that would be released if no Tu-GDP dissociation occurred. The difference curve (c − {b + d}) is a measure of the GTPase associated with monomer−polymer exchange reactions. Samples for determination of microtubule number concentration were taken at the times indicated by the arrows. See text for full details.

Self-Assembly. Figure 3 shows a typical self-assembly experiment in which Tu-GTP (C_t = 30 μM) and MDCC−PBP (90 μM) in PEMG buffer were added to a cuvette which had been prewarmed to 37 °C. The initial decrease in fluorescence signal (t = 0−70 s, curve a) is due to the effect of changing temperature. For the comparison of the P_i curve and the polymer mass curve (curve b), the former needs to be corrected for the background P_i present at t = 0. In principle this could be done by subtracting the P_i signal at the time where thermal equilibrium is attained (e.g., 11.7 μM at t = 70 s). This also subtracts any P_i produced over the first 70 s by the intrinsic GTPase and by nucleation events. The amount of P_i produced through the intrinsic GTPase has been calculated (see Materials and Methods) and is shown as curve d; this is a somewhat approximate calculation since it neglects the effects of the temperature change occurring at short times and ignores the fact that k_{Int} is greater than 2.9 × 10^{-4} s^{-1} at high C_t (see above). Nevertheless, the amount of P_i produced at t = 70 s is estimated to be approximately 0.7 μM and the background P_i is therefore estimated to be ∼11 μM. The P_i release curve corrected for this background (curve c) clearly illustrates that P_i release exceeds polymer formation under these conditions. If no Tu-GDP dissociation occurs during the assembly process, then the total amount of P_i released is equal to the amount of Tu-GTP incorporated into the polymer (assuming all GTP to be hydrolyzed) plus that produced though the intrinsic hydrolysis reaction (i.e., the sum of curves b and d, indicated as curve {b + d} in Figure 3). Curves c and {b + d} clearly superimpose at short times; thus elongation is

highly efficient in the sense that Tu-GDP dissociation events are rare during rapid elongation. At longer times total P_i production exceeds the sum {b + d}. The difference curve (curve labeled c − {b + d}) then represents P_i produced by dynamic instability, and the slope of the linear portion of this curve is therefore $R_{Pi,DI}$ (see Materials and Methods and below).

Seeded Assembly. Seeded assembly has been used to avoid contributions to P_i release during the nucleation phase of self-assembly. Figure 4A shows a typical seeded assembly experiment in which polymer formation and P_i production were monitored over approximately 1 h. Tu-GTP (16 μM) and MDCC−PBP (80 μM) were added to a prewarmed cuvette (37 °C), and 0.5 μM polymerized tubulin (as seeds) was added (t = 150 s) when thermal equilibrium had been attained. There is an instantaneous small increase in polymer mass, due to the seeds, and in the P_i signal, from background P_i in the seed preparation. Control experiments in which seeds were added to a buffer solution containing no Tu-GTP showed that the P_i background exceeded the concentration of polymerized tubulin present in the seed preparation (see below). Samples for the determination of microtubule number concentration (C_n) were taken at the times indicated by the arrows. C_n decreased from 0.54 ± 0.12 nM at t = 1500 s to 0.38 ± 0.08 nM at t = 3600 s. Changes in microtubule number concentration of this magnitude clearly preclude the use of eq 3 in the kinetic analysis of P_i release curves at longer times after establishment of the steady state.

Figure 4B shows a fast seeded assembly in which 1.5 μM polymerized tubulin (as seeds) was added (at t = 70 s) to 26.0 μM Tu-GTP. The microtubule number concentration determined at the end of the elongation phase was 2.3 ± 0.7 nM. For seeded assemblies one is only concerned with P_i produced from the point at which the seeds are added. The corrected P_i curve (curve c) is therefore given by subtracting the signal immediately prior to the addition of seeds (original background P_i) plus the *excess* P_i (i.e., total P_i minus concentration of tubulin present as seeds) contained in the seed preparation. The intrinsic GTPase (calculated from the point of seed addition) is shown as curve d; the low amplitude of this curve shows that only small amounts of P_i are produced through this reaction under these conditions, since the soluble tubulin is rapidly depleted by the fast assembly. It is clear that the corrected P_i production curve (curve c) and the sum curve {b + d} (equal to the amount of P_i that would be produced during microtubule assembly if Tu-GDP dissociation events did not occur; see above) superimpose over most of the elongation phase of assembly, consistent with the view that GTP hydrolysis is closely coupled to Tu-GTP addition under these conditions. The difference curve (c − {b + d}) was again used to assess the amount of P_i produced by monomer−polymer exchange reactions at the steady state of assembly. This curve becomes nonlinear at long times because of changes in microtubule number concentration (see Figure 4A).

A similar analysis for a slow seeded assembly ([Tu-GTP] = 16, 0.2 μM polymerized tubulin added as seeds) is shown in Figure 4C; in this case, the microtubule number concentration determined at the end of the elongation phase was 0.32 ± 0.06 nM. In this case the corrected P_i release (c) runs ahead of the sum curve ({b + d}) almost from the onset of assembly. This suggests that, under conditions of very slow growth, there are substantial numbers of Tu-GDP dissociation events occurring throughout the elongation phase. The difference curve (c − {b + d}) can again be used to assess the steady-state GTPase associated with dynamic instability. In this case it is more difficult to determine the slope since the curve shows a significant lag (because Tu-GDP dissociation events are less common in the early stages of assembly) followed by a deviation from linearity at long times (due to changes in microtubule number concentration). For this particular experiment the slope was taken between 1000 and 1500 s.

The Steady-State GTPase. Values of k_{obs} for assembly curves obtained from light-scattering traces were determined from eq 1 using microtubule number concentrations determined close to the end of the elongation phase. These k_{obs} values are plotted as a function of C_n in Figure 5A. The significant scatter in these data is primarily associated with the errors in the determination of C_n (typically 15−25%; see above). Nevertheless, linear regression to the equation $k_{obs} = k_a C_n$ yields an effective bimolecular association rate constant for the addition of Tu-GTP to microtubule ends (k_a) of 8.1 (±0.4) × 10^6 M^{-1} s^{-1}, in good agreement with previous estimates (*10*, *13*, *40*, *42*).

The correlation between the steady-state GTPase associated with monomer−polymer exchange reactions ($R_{Pi,DI}$, determined as described above) and the microtubule number concentration was also examined (Figure 5B). The slope of this plot should be equal to $k_a f_G C_c$ (see Materials and Methods). The solid line was calculated using f_G = 0.9 (see Materials and Methods), and the values of k_a and C_c determined as described above (the dotted lines are the limiting slopes calculated using the error limits determined for k_a and C_c). The agreement between the experimental and calculated values confirms that P_i production at the steady state is largely attributable to dynamic length excursions under these conditions.

The Effects of GDP. It is well-established that Tu-GDP is able to coassemble with Tu-GTP into microtubules (*12*, *38*, *43*). The presence of Tu-GDP contamination in the Tu-GTP solutions used in experiments such as those described here could therefore create the impression that hydrolysis is "delayed" relative to assembly (cf. ref *41*). This is because the incorporation of Tu-GDP into the microtubules would contribute to the light-scattering signal but not to the fluorescence signal. To evaluate the effect of direct incorporation of Tu-GDP into microtubules, we have performed seeded assemblies in the presence of known amounts of Tu-GDP, using appropriate GTP/GDP mixtures to control the levels of Tu-GDP (*38*).

Figure 6 shows a typical experiment carried out under conditions where 20% of the tubulin contained (E-site) GDP. These curves demonstrate that P_i production (corrected for P_i background, curve c) does indeed appear to be delayed relative to assembly (curve b). The amount of P_i produced through the intrinsic hydrolysis reaction is predicted to be very small (curve d) under these rapid assembly conditions. The possibility that the intrinsic hydrolysis rate may be higher in the presence of Tu-GDP (*41*) has not been considered, but we note that even a very substantial enhancement would not make this contribution significant under these conditions. The difference curve (c − {b + d}) has been used to assess the steady-state GTPase associated with monomer−polymer

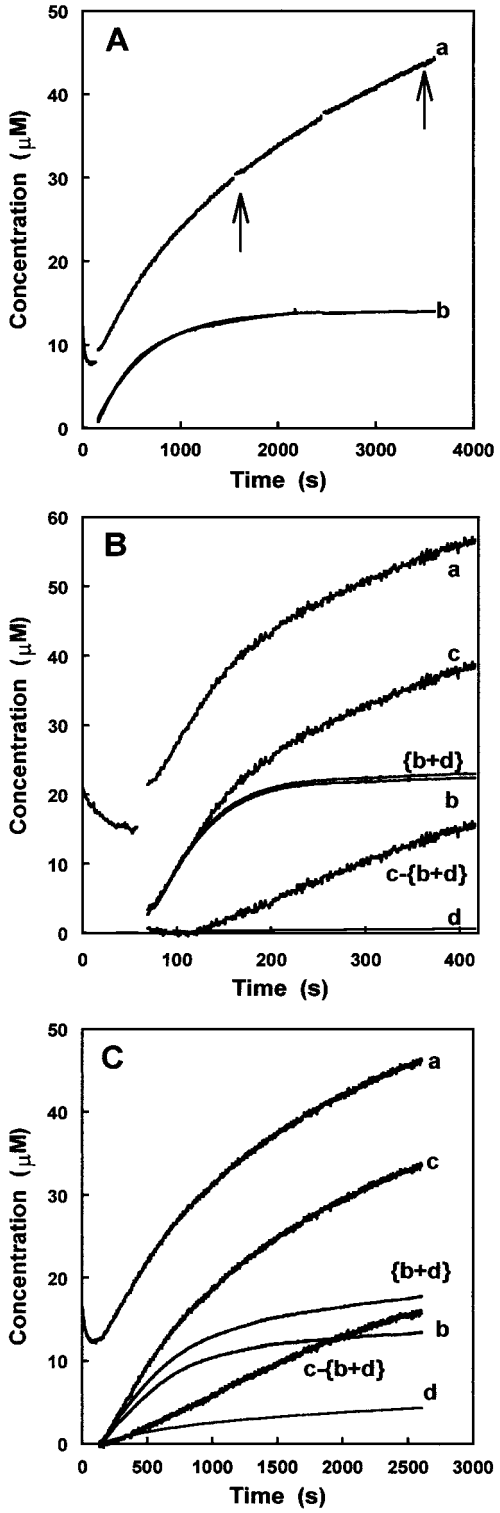

FIGURE 4: P_i release under seeded assembly conditions. Fluorescence and light-scattering signals were monitored following the addition different concentrations of polymerized tubulin (as seeds) to Tu-GTP, MDCC−PBP (60−90 μM), and excess GTP (250−350 μM) in PEMG buffer (at 37 °C): (A) 0.5 μM tubulin (as seeds) added to 16.0 μM Tu-GTP; (B) 1.5 μM tubulin (as seeds) added to 25.0 μM Tu-GTP; and (C) 0.2 μM tubulin (as seeds) added to 16.0 μM Tu-GTP. The curves are labeled as follows: (a) measured P_i concentration; (b) concentration of tubulin present as polymer (C_p); (c) P_i release curve (curve a corrected for P_i background); and (d) P_i production from the intrinsic GTPase of Tu-GTP. The sum curve ({b + d}) represents the amount of P_i that would be released if no Tu-GDP dissociation occurred. The difference curve (c − {b + d}) is a measure of the GTPase associated with monomer−polymer exchange reactions. See text for full details.

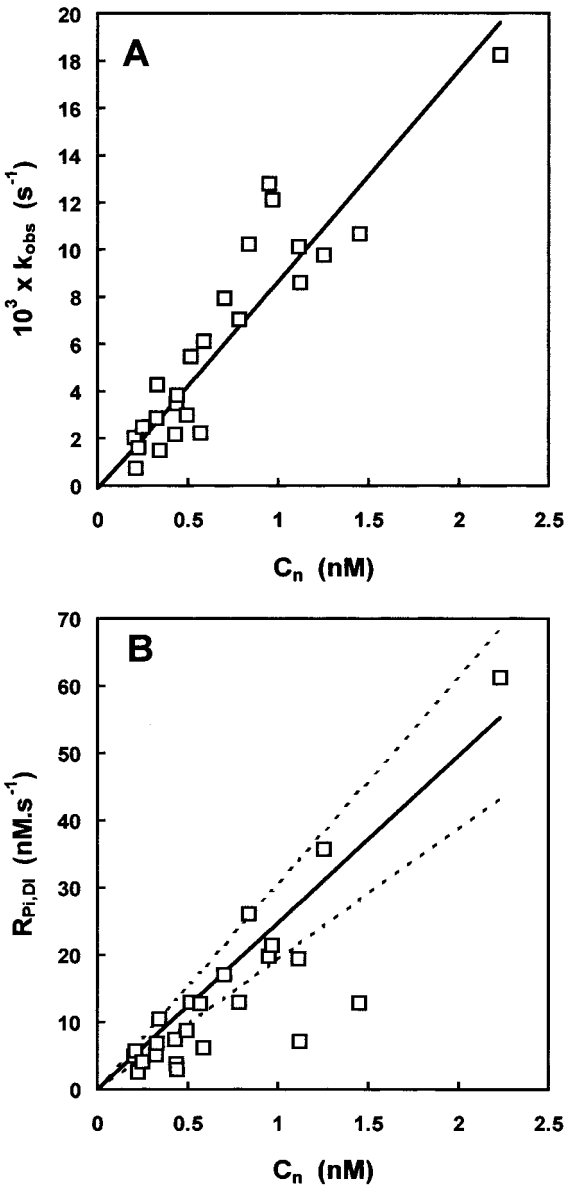

FIGURE 5: The GTPase associated with monomer−polymer exchange reactions. (A) Values of k_{obs} determined from scatter curves plotted as a function of C_n. The slope corresponds to an effective bimolecular rate constant for the addition of Tu-GTP to microtubule ends of 8.1 (± 0.4) × 10^6 M^{-1} s^{-1}. (B) Values of $R_{Pi,DI}$ plotted as a function of C_n. The solid line corresponds to the expected dependence based on the equation $R_{Pi,DI} = k_a f_G C_c C_n$ using $f_G = 0.9$ and the values of C_c and k_a determined in Figures 1 and 5A, respectively. The dotted lines represent estimated error limits (see text).

exchange reactions. The negative region of this curve over the elongation period (150−400 s) is attributable to the amount of Tu-GDP incorporated, but this has not been quantitated.

The results from a series of experiments carried out at 0%, 10%, 20%, and 40% Tu-GDP are summarized in Table 1. The present results confirm those of a previous study (*38*) carried out in PEM buffer (no glycerol) in which it was shown that Tu-GDP at up to 40% had only a small effect on the apparent critical concentration. We show here that the presence of 40% Tu-GDP reduces the effective bimolecular association rate constant (k_a) by no more than 30−40% compared with the control value, confirming the previous

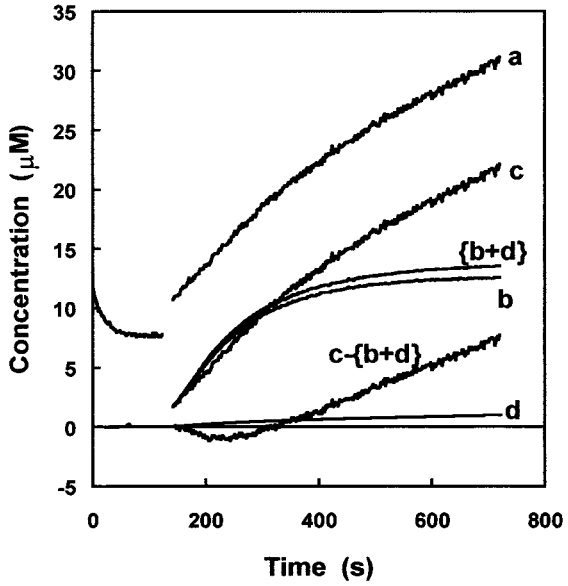

FIGURE 6: The effect of Tu-GDP on P_i release during microtubule assembly. Fluorescence and light-scattering signals were monitored following the addition of 1.5 μM polymerized tubulin (as seeds) to tubulin (16 μM with [Tu-GDP]/([Tu-GDP] + [Tu-GTP]) = 0.2), MDCC−PBP (80 μM), and excess GTP/GDP (235/176 μM) in PEMG buffer (at 37 °C). The curves are labeled as follows: (a) measured P_i concentration; (b) concentration of tubulin present as polymer (C_p); (c) P_i release curve (curve a corrected for P_i background); and (d) P_i production from the intrinsic GTPase of Tu-GTP. The sum curve ({b + d}) represents the amount of P_i that would be released if no Tu-GDP dissociation occurred. The difference curve (c − {b + d}) is a measure of the GTPase associated with monomer−polymer exchange reactions. See text for full details.

Table 1: Parameters for Seeded Assembly Carried out in the Presence of Different Concentrations of Tu-GDP

fraction of Tu-GDP	C_c (μM)[a]	C_n (nM)	$10^3 \times k_{obs}$ (s^{-1})[b]	$10^6 \times k_a$ ($M^{-1}\ s^{-1}$)[c]	$R_{Pi,DI}$ (nM s^{-1})[d]
0	3.4 (0.6)	0.79 (0.24)	8.20 (0.1)	10.40 (4.0)	23.8 (1.4)
0.1	4.2 (0.7)	0.84 (0.27)	7.45 (0.15)	8.90 (4.5)	20.3 (1.3)
0.2	5.0 (0.8)	0.76 (0.24)	6.60 (0.1)	8.70 (4.0)	19.6 (1.2)
0.4	6.9 (1.2)	0.72 (0.23)	5.15 (0.15)	7.15 (3.5)	13.9 (1.7)

[a] Determined as described in Materials and Methods. [b] Determined from analysis of light-scattering data. [c] k_a is calculated as $k_{obs}/\mathbf{C_n}$. [d] Determined as described in the text.

observation that growth rates of individual microtubules were also relatively unaffected by the presence of these concentrations of Tu-GDP (*38*). Finally, Table 1 shows that the steady-state GTPase associated with monomer−polymer exchange is also reduced by some 40% in the presence of 40% Tu-GDP.

The Effects of Cytostatic Drugs. We have used MDCC−PBP to investigate the effects of two drugs (podophyllotoxin and 2-methoxy-5-(2′,3′,4′-trimethoxyphenyl) tropone (MTC, a fast-acting colchicine analogue)) added to microtubules during the fast elongation phase of assembly. Large concentrations of podophyllotoxin induce complete microtubule disassembly (*44*), while small concentrations of MTC inhibit microtubule elongation without necessarily inducing microtubule disassembly, and accelerate tubulin's intrinsic GTPase (*45*, *46*). Figure 7A shows an assembly initiated by the addition of 1.5 μM polymerized tubulin (as seeds) to 16 μM Tu-GTP. At the point indicated by the arrow, 290 μM

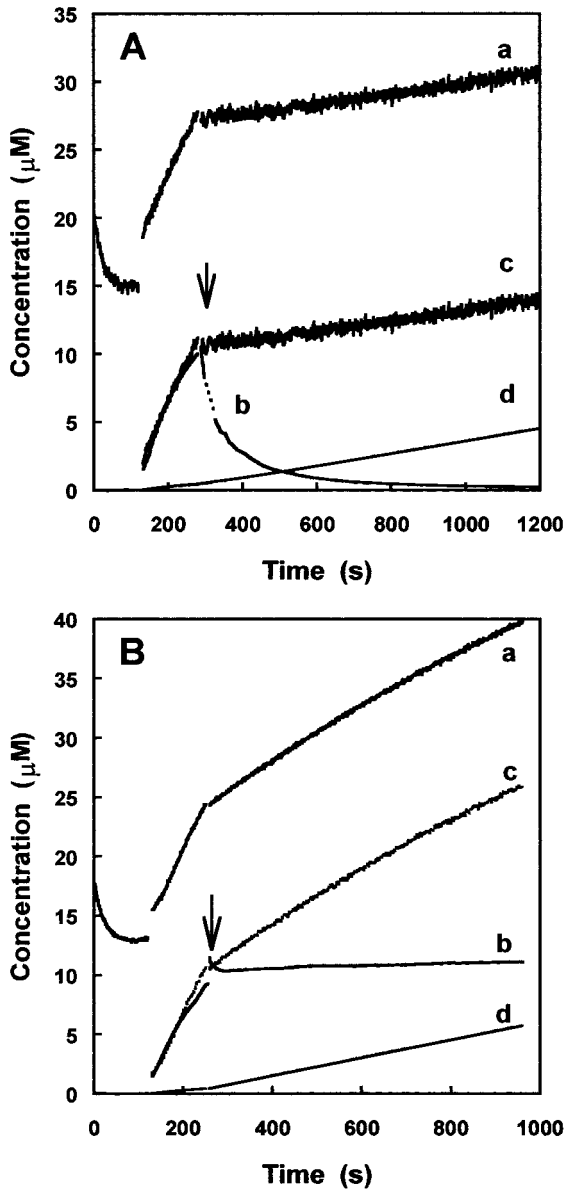

FIGURE 7: The effect of cytostatic drugs on P_i release during microtubule assembly. Fluorescence and light-scattering signals were monitored following the addition of 1.5 μM polymerized tubulin (as seeds) to Tu-GTP (16 μM), MDCC−PBP (80 μM), and excess GTP (250 μM) in PEMG buffer (at 37 °C). At the point indicated by the arrow the cytostatic drug was added: (A) 290 μM podophyllotoxin and (B) 1.4 μM MTC. The curves are labeled as follows: (a) measured P_i concentration; (b) concentration of tubulin present as polymer (C_p); (c) P_i release curve (curve a corrected for P_i background); and (d) P_i production from the intrinsic GTPase of Tu-GTP and the Tu-GTP−drug complex. Podophyllotoxin had no effect on k_{Int}; in contrast, MTC lead to a greatly enhanced intrinsic GTPase. Thus, in Figure 7B we have used a rate of 6 nM s^{-1} for 1.4 μM Tu-GTP-MTC.

podophyllotoxin was added to induce microtubule disassembly. The scatter signal (curve b) disappeared rapidly as microtubules disassembled, while P_i release continued at a greatly reduced, but apparently steady, rate (curve c). The important point here is that the addition of podophyllotoxin did not cause a burst in the P_i signal, the expected behavior if significant amounts of P_i (more than a few percent of polymer mass) had been retained in the growing microtubule. Curve d shows a calculation of the amount of P_i expected to be produced through the intrinsic GTPase of tubulin. The

rate of P_i production through this process increases, due to the increase in soluble tubulin, released by the disassembling microtubules.

Figure 7B shows a similar experiment in which 1.4 μM MTC was added at the point indicated by the arrow. The addition of MTC inhibits microtubule elongation but does not cause microtubule disassembly; the polymer mass signal (curve **b**) therefore remains constant after the addition of the drug. In contrast, P_i release continues at a significant rate (curve c). This is partly attributable to the high rate of the intrinsic GTPase of the Tu-GTP−MTC complex; curve d shows a calculation of the amount of P_i expected to be produced through the intrinsic GTPase reaction of free Tu-GTP plus that of Tu-GTP-MTC (see figure legend). This clearly does not account for all of the P_i produced following addition of the drug, suggesting that Tu-GDP is still being produced at a significant rate even though net elongation is totally blocked by the MTC.

DISCUSSION

We have examined the assembly of Tu-GTP under conditions which support microtubule dynamic instability (i.e., low [Mg^{2+}], 1 M glycerol, and no MAPs or taxol). Using MDCC−PBP to monitor P_i allows a continuous direct assay of P_i without recourse to sampling, and at 0.2 s intervals, the measurement can be switched between fluorescence and 90° light scattering, to provide effectively simultaneous records of the two parameters (*32*). Conditions were chosen such that the maximum saturation of MDCC−PBP is <70% to maintain a linear response (*33*). High assembly rates were obtained by using high microtubule number concentrations for a given tubulin concentration. The experimental variability of the 90° light-scattering signal requires internal calibration of the polymer mass using knowledge of C_t and C_c (see Materials and Methods).

As with much of the earlier work in this area the method shares the problem of having to relate two different kinds of observations made in the micromolar tubulin concentration range, with processes in microtubules which are only present at the nanomolar number concentration. This situation is aggravated by the fact that the P_i-related signal originates from two processes which differ in importance at different stages of assembly, namely GTP hydrolysis associated with polymer formation, and that associated with tubulin in solution. This work clearly shows that the latter contribution is not negligible, especially under conditions of slow assembly (See Figures 3 and 4C), and in the presence of drugs which can increase the intrinsic hydrolysis rate (e.g. MTC, see Figure 7B). At the steady state of assembly (C_c = 3.4 μM) the intrinsic GTPase of soluble tubulin is ~1 nM s^{-1} (see Figure 2B), whereas P_i production deriving from microtubule elongation varies from 5 to 50 nM s^{-1}, depending on the number concentration (C_n = 0.2−2 nM) (see Figure 5B).

The results show that P_i production can readily exceed microtubule assembly in self-nucleated assemblies (Figure 3) and under conditions of slow seeded assembly (Figure 4C), due to the intrinsic GTPase of Tu-GTP. More generally, with higher assembly rates, the initial production of P_i in nucleated assembly closely follows microtubule assembly, suggesting that Tu-GTP or Tu-GTP−P_i species can only be a (very) small fraction of the polymerized tubulin. These observations are in agreement with numerous observations (see Introduction), which demonstrate that little, if any, of the microtubule polymer mass consists of Tu-GTP under the conditions of such experiments.

The dependence of k_{obs} (determined from light-scattering curves) on the microtubule number concentration gives (Figure 5A) an average bimolecular association rate constant, k_a, of 8.1 × 10^6 M^{-1} s^{-1}, in good agreement with previous estimates (*10*, *13*, *40*, *42*). The rate of P_i production associated with microtubule elongation during periods of growth at the steady state (Figure 5B) follows the predicted dependence on k_a, C_n, and C_c, given the assumption of tight coupling between microtubule elongation reactions and the release of P_i following GTP hydrolysis.

The results in Figure 7B show that sudden inhibition of microtubule assembly with a cytostatic drug (MTC) shows no evidence for the accumulation of P_i in the microtubule lattice; the release of P_i is inhibited, together with the inhibition of fast microtubule elongation. The sudden disassembly of rapidly growing microtubules induced by the addition of podophyllotoxin did not produce a sudden burst of P_i in solution. This latter result argues persuasively that there is normally little or no P_i retained in the lattice even during fast growth.

In conclusion, the present work supports earlier reports that Tu-GTP is not being accumulated in the microtubule lattice during periods of fast growth (*13*, *15*−*19*). The possibility that a substantial part of the ends may consist of Tu-GDP−P_i (*14*, *26*, *47*) is not supported. The absence of stabilizing effects of P_i on microtubules (reviewed in ref *43*) suggests that the species Tu-GDP−P_i, which must be present at least as a transient intermediate in GTP hydrolysis, behaves kinetically more like Tu-GDP than Tu-GTP. Thus, little or no influence might be expected on microtubule dynamics (*25*, *48*).

So what stabilizes a growing microtubule? This question can be approached in two somewhat distinct ways, structural and kinetic. Regarding the structural approach, the molecular understanding has been greatly enhanced by the elucidation of the structure of the tubulin $\alpha\beta$-heterodimer at atomic resolution (*49*). This clearly locates the β subunit (E-site) GTP close to the interface with the α subunit, and the E-site would then be exposed, especially at the "β-out" end. It appears most probable that the formation of the $\alpha\beta$ interface between adjacent tubulin dimers in the microtubule lattice is structurally linked to GTP hydrolysis. Also, Chrétien and co-workers (*50*−*52*) using frozen hydrated specimens, have shown the existence at the end of microtubules of incomplete sheetlike structures, comprising a number of protofilaments. These workers have postulated that the rate of closure of these into complete (cylindrical) lattices, which could depend on their size, could determine the kinetic properties of microtubule ends. Recently, Janosi et al. (*51*) have modeled the elastic properties of microtubule sheets and walls and shown that the three-dimensional curvature of sheets growing off of a cylindrical lattice may be strongly dependent on the number of protofilaments in the sheets. Such structures can involve several hundred tubulin monomers, certainly exceeding the number visualizable by fluorescence microscopy and approaching the level detectable by biochemical assay. If the sheets were composed of Tu-GTP, then concerted

hydrolysis correlating with the closure reaction would be required. If the sheets were composed of Tu-GDP, then they might be expected to be inherently unstable. In fact, the biochemical composition of the sheetlike structure is presently unknown.

Regarding the kinetic approach, we have previously presented in the lateral cap model (*25*) the general limiting case in which the addition of Tu-GTP is coupled directly to the hydrolysis of a longitudinally adjacent Tu-GTP molecule (in either A- or B-type microtubule lattices). This produces the minimal cap with a single lateral terminal layer of bound Tu-GTP in the growing state. Computer simulation shows that the appropriate choice of kinetic constants for this model can reproduce the basic phenomena of microtubule dynamic instability, namely random transitions between growing and shortening states; strong dependence of state lifetimes on the concentration of nonpolymerized Tu-GTP; characteristic properties at the two ends; and specific effects of GDP, drugs, and MAPs (*25*, *38*, *42*, *44*, *46*). The stabilization of the growing microtubule occurs because of the differential kinetic properties of bound Tu-GTP and Tu-GDP. Some experimental confirmation of such a minimal single layer cap also comes from the work of Drechsel and Kirschner (*20*). However, the lateral cap model represents the limiting case of fast hydrolysis. It is clear that hydrolysis of bound Tu-GTP must occur on a finite time scale, and it may be tubulin isotype and species-specific (cf. ref *31*). Hence at sufficiently high [Tu-GTP], the bimolecular addition rate can approach or exceed this limit, and then the bound Tu-GTP will accumulate. The present work suggests that hydrolysis can keep pace with addition rates of 200 tubulins per second per microtubule. With C_c normally in the range 2−5 μM and a k_a of the order of 8×10^6 M^{-1} s^{-1} (i.e., 16−40 tubulins per second per microtubule), it is unlikely that dynamic instability, which occurs at concentrations in the region of C_c, involves the build-up of significant bound Tu-GTP caps.

Thus the detailed relationship between the kinetic results and the structural information is still not resolved. It is possible that the terminal sheet structures of growing microtubules are composed of Tu-GDP, curved protofilaments of which might remain relatively stable, with the structural transition to the normal microtubule lattice conferring the potential instability characteristic of the Tu-GDP microtubule. Alternatively, their extremities (i.e., the longitudinal edges as well as the lateral surface) might be composed of bound Tu-GTP molecules, with kinetic properties sensitive to their neighboring lattice interactions, similar to what has been postulated for terminal Tu-GTP in the lateral cap model (*25*). Thus the final link in the question of stabilization of growing microtubules may depend on clarification of the detailed relationship between the topology and the biochemical content (Tu-GTP versus Tu-GDP) of the terminal structures.

ACKNOWLEDGMENT

We thank Mrs. Jackie Hunter (NIMR, London) for preparation of the phosphate binding protein and Prof. Yves Engelborghs (Katholieke Universiteit te Leuven, Belgium) for providing us with MTC.

REFERENCES

1. Avila, J. (1990) *FASEB J. 4*, 3284−3290.
2. Dustin, P. (1978) *Microtubules*, Springer-Verlag, Berlin, Germany.
3. Hyams, J. S., and Lloyd, C., Eds. (1994) *Microtubules*, Wiley-Liss, New York.
4. Mitchison, T., and Kirschner, M. (1984) *Nature 312*, 232−237.
5. Horio, T., and Hotani, H. (1986) *Nature 321*, 605−607.
6. Pantaloni, D., and Carlier, M.-F. (1986) *Ann. N. Y. Acad. Sci. 466*, 496−509.
7. Caplow, M., Ruhlen, R. L., and Shanks, J. (1994) *J. Cell Biol. 127*, 779−788.
8. Hyman, A. A., Salser, S., Drechsel, D. N., Unwin, N, and Mitchison, T. J. (1992) *Mol. Biol. Cell 3*, 1155−1167.
9. Carlier, M.-F., Hill, T. L., and Chen, Y. (1984) *Proc. Natl. Acad. Sci. U.S.A. 81*, 771−775.
10. Walker, R. A., O'Brien, E. T., Pryer, N. K., Sobeiro, M., Voter, W. A., Erickson, H. P., and Salmon, E. D. (1988) *J. Cell. Biol. 107*, 1437−1448.
11. Carlier, M.-F., and Pantaloni, D. (1981) *Biochemistry 20*, 1918−1924.
12. Carlier, M.-F., Didry, D., and Pantaloni, D. (1987) *Biochemistry 26*, 4428−4437.
13. Stewart, R. J., Farrell, K. W., and Wilson, L. (1990) *Biochemistry 29*, 6489−6498.
14. Melki, R., Fievez, S., and Carlier, M.-F. (1996) *Biochemistry 35*, 12038−12045.
15. Hamel, E., del Campo, A. A., Lowe, M. C., Waxman, P. G., and Lin, C. M. (1982) *Biochemistry 21*, 503−509.
16. O'Brien, E. T., Voter, W. A., and Erickson, H. P. (1987) *Biochemistry 26*, 4148−4156.
17. O'Brien, E. T., Salmon, E. D., Walker, R. A., and Erickson, H. P. (1990) *Biochemistry 29*, 6648−6656.
18. Schilstra, M. J., Martin, S. R., and Bayley, P. M. (1987) *Biochem. Biophys. Res. Commun. 147*, 588−595.
19. Walker, R. A., Pryer, N. K., and Salmon, E. D. (1991) *J. Cell Biol. 114*, 73−81.
20. Drechsel, D. N., and Kirschner, M. W. (1994) *Curr. Biol. 4*, 1053−1061.
21. Caplow, M., and Shanks, J. (1996) *Mol. Biol. Cell 7*, 663−675.
22. Chen, Y., and Hill, T. L. (1985) *Proc. Natl. Acad. Sci. U.S.A. 82*, 1131−1135.
23. Bayley, P. M., Schilstra, M. J., and Martin, S. R. (1989) *J. Cell Sci. 93*, 241−254.
24. Bayley, P. M., Schilstra, M. J., and Martin, S. R. (1990) *J. Cell Sci. 95*, 33−48.
25. Martin, S. R., Schilstra, M. J., and Bayley, P. M. (1993) *Biophys. J. 65*, 578−596.
26. Melki, R., Carlier, M.-F., and Pantaloni, D. (1990) *Biochemistry 29*, 8921−8932.
27. Carlier, M.-F., Didry, D., Simon, C., and Pantaloni, D. (1989) *Biochemistry 28*, 1783−1791.
28. Caplow, M., Ruhlen, R., Shanks, J., Walker, R. A., and Salmon, E. D. (1989) *Biochemistry 28*, 8136−8141.
29. Trinczek, B., Marx, A., Mandelkow, E.-M., Murphy, D. B., and Mandelkow, E. (1993) *Mol. Biol. Cell 4*, 323−335.
30. Caplow, M., and Shanks, J. (1998) *Biochemistry 37*, 12994−13002.
31. Dougherty, C. A., Himes, R. H, Wilson, L., and Farrell, K. W. (1998) *Biochemistry 37*, 10861−10865.
32. Brune, M., Hunter, J. L., Corrie, J. E. T., and Webb, M. R. (1994) *Biochemistry 33*, 8262−8271.
33. Brune, M., Hunter, J. L., Howell, S. A., Martin, S. R., Hazlett, T. L., Corrie, J. E. T., and Webb, M. R. (1998) *Biochemistry 37*, 10370−10380.
34. Shelanski, M. L., Gaskin, F., and Cantor, C. R. (1973) *Proc. Natl. Acad. Sci. U.S.A. 70*, 765−768.
35. Weingarten, M. D., Lockwood, A. H., Hwo, S. Y., and Kirschner, M. W. (1975) *Proc. Natl. Acad. Sci. U.S.A. 72*, 1858−1862.
36. Engelborghs, Y., Dumortier, C., D'Hoore, A., Vandecandelaere, A., and Fitzgerald, T. J. (1993) *J. Biol. Chem. 268*, 107−112.
37. Bradford, M. M, (1976) *Anal. Biochem. 72*, 248−254.

38. Vandecandelaere, A., Martin, S. R., and Bayley, P. M. (1995) *Biochemistry 34*, 1332−1343.
39. Caplow, M., and Shanks, J. (1990). *J. Biol. Chem. 265*, 8935−8941.
40. Symmons, M. F., Martin, S. R., and Bayley, P. M. (1996) *J. Cell Sci. 109*, 2755−2766.
41. Carlier, M.-F., Didry, D., and Pantaloni, D. (1997) *Biophys. J. 73*, 418−427.
42. Vandecandelaere, A., Pedrotti, B., Utton, M.A., Calvert, R. A., and Bayley, P. M. (1996) *Cell Motil. Cytoskeleton 35*, 134−146.
43. Caplow, M., and Shanks, J. (1995) *Biochemistry 34*, 15732−15741.
44. Schilstra, M. J., Martin, S. R., and Bayley, P. M. (1989) *J. Biol. Chem. 264*, 8827−8834.
45. Perez-Ramirez, B., Andreu, J. M., Gorbunoff, M. J., and Timasheff, S. N. (1996) *Biochemistry 35*, 327−3285.
46. Vandecandelaere, A., Martin, S. R., and Engelborghs, Y. (1997) *Biochem. J. 323*, 189−196.
47. Carlier, M.-F., Didry, D., Melki, R., Chabre, M., and Pantaloni, D. (1988) *Biochemistry 27*, 3555−3559.
48. Bayley, P. M., Sharma, K. K., and Martin, S. R. (1994) in *Microtubules* (Hyams, J. S., and Lloyd, C., Eds.) pp 111−137, Wiley-Liss, New York.
49. Nogales, E., Wolf, S. G., and Downing, K. H. (1998) *Nature 391*, 199−203.
50. Chrétien, D., Fuller, S. D., and Karsenti, E. (1995) *J. Cell Biol. 129*, 1311−1328.
51. Janosi, I. M., Chrétien, D., and Flyvberg, H. (1998) *Eur. Biophys. J. 27*, 501−513.
52. Muller-Reichert, T., Chrétien, D., Severin, F., and Hyman, A. A. (1998) *Proc. Natl. Acad. Sci. U.S.A. 95*, 3661−3666.

BI9830765